THE INTERNATIONAL JOURNAL OF
DEVELOPMENTAL BIOLOGY
www.intjdevbiol.com

Dissecting the neural divide: a continuous neurectoderm gives rise to the olfactory placode and bulb

JORGE TORRES-PAZ[1], EUGENE M. TINE[2,3] and KATHLEEN E. WHITLOCK*[,2,3]

[1]Université Paris-Saclay, CNRS, Institut des Neurosciences Paris-Saclay, Gif-sur-Yvette, France,
[2]Centro Interdisciplinario de Neurociencia de Valparaíso (CINV), Universidad de Valparaíso, Valparaíso, Chile and
[3]Instituto de Neurociencia, Universidad de Valparaíso, Valparaíso, Chile and

ABSTRACT **The olfactory epithelia arise from morphologically identifiable structures called olfactory placodes. Sensory placodes are generally described as being induced from the ectoderm, suggesting that their development is separate from the coordinated cell movements generating the central nervous system. Previously, we have shown that the olfactory placodes arise from a large field of cells bordering the telencephalic precursors in the neural plate, and that cell movements, not cell division, underlie olfactory placode morphogenesis. Subsequently by image analysis, cells were tracked as they moved in the continuous sheet of neurectoderm, giving rise to the peripheral (olfactory organs) and central (olfactory bulbs) nervous system (Torres-Paz and Whitlock, 2014). These studies lead to a model in which the olfactory epithelia develop from within the border of the neural plate and are a neural tube derivative, similar to the retina of the eye (Torres-Paz and Whitlock, 2014; Whitlock, 2008). Here, we show that randomly generated clones of cells extend across the morphologically differentiated olfactory placodes/olfactory bulbs, and test the hypothesis that these structures are patterned by a different level of *distal-less (dlx)* gene expression, subdividing the anterior neurectoderm into olfactory placode precursors (high Dlx expression) and olfactory bulb precursors (lower Dlx expression). Manipulation of DLX protein and RNA levels resulted in morphological changes in the size of the olfactory epithelia and olfactory bulb. Thus, the olfactory epithelia and bulbs arise from a common neurectodermal region and develop in concert through coordinated morphological movements.**

KEY WORDS: *lineage, telencephalon, retina, distal-less, emx1, emx3*

Introduction

Precise communication between peripheral nervous system (PNS) and central nervous system (CNS) is essential for coordinated neural activity necessary to relay sensory information to the brain. The coordination of gene expression during early embryogenesis controls the differentiation of cells giving rise to the PNS and CNS, thus ensuring the assembly of functional sensory modules. In vertebrates, the CNS arises from the neural ectoderm through primary or secondary neurulation the details dependent upon the organism. In contrast the PNS is thought to arise from regions of thickened ectodermal tissue called sensory placodes originally identified as focal thickenings of tissue histological preparations (Jacobson, 1966; Johnston, 1909; Klein and Graziadei, 1983).

Our previous work supports the origin of the olfactory placode as the border of the neural plate, i.e. neurectoderm (Whitlock and Westerfield, 2000) (Harden *et al.*, 2012; Torres-Paz and Whitlock, 2014). The neural plate border is initially specified during late blastula /early gastrula by interactions between BMP and FGF, then maintained through gastrulation by BMP and Wnt signaling that continue to interact with FGF to maintain neural identity at the end of gastrulation in the neural plate (Schille and Schambony, 2017) (Patthey and Gunhaga, 2014) (Schlosser *et al.*, 2014). Thus non-neural fates must be defined, as evidenced by BMP4 activity

---

Abbreviations used in this paper: BMP, bone morphogenetic protein; dlx, distal-less gene; FGF, fibroblast growth factor; OB, olfactory bulb; OE, olfactory epithelium; OP, olfactory placode; PNS peripheral nervous system.

***Address correspondence to:** Kathleen Whitlock. Centro Interdisciplinario de Neurociencia de Valparaíso (CINV), Universidad de Valparaíso, Valparaíso, Chile and Instituto de Neurociencia, Universidad de Valparaíso, Valparaíso, Chile. Pasaje Harrington 287, Valparaíso, Chile. Tel: 32-299-5510, 32-250-8040. Fax: 32-250-8027. E-mail: kathleen.whitlock@uv.cl - (iD) https://orcid.org/0000-0002-2677-4368

required for the differentiation of lens but not olfactory placode (OP) cells (Chapman *et al.*, 2002) (Sjodal *et al.*, 2007), after the initial specification of neural progenitors in the neural plate border during blastula/gastrula stages (See for review Patthey and Gunhaga, 2014, Fig. 1).

Once morphologically apparent the sensory placodes give rise to diverse structures such as the lens of the eye (but not the retina), the inner ear, the olfactory epithelium (OE) and the cranial ganglia (Patthey *et al.*, 2014; Schlosser, 2006). The sensory placodes generating this heterogeneous collection of cell types are described as to arising from a common base-state, the "pre-placode domain". This domain is defined based on patterned gene expression at the edge of the neural plate at the end of gastrulation (Pieper *et al.*, 2011; Schlosser, 2006). The model whereby the placodal precursors segregate from a common cellular field in the transition between neural and non-neural ectoderm at the end of gastrulation tends to gloss over fundamental developmental and evolutionary differences in placodes. Most importantly the oversimplification of the placodes as derivatives of naïve ectoderm with competence to respond to appropriate inductive signals, ignores the process by which placodes have co-evolved with their developmental partners in the neural tube. In the case of the olfactory placode this is essential to consider because the first synapse lies within the central nervous system (CNS) thus evolutionary forces must keep the peripheral and central components in register.

In contrast to other sensory neurons, the photoreceptors in the retina are the only sensory cells in the anatomically defined peripheral nervous system (PNS) derived from the neural plate; the receptors of the other sensory modalities (olfaction, hearing, taste, touch) are derived from placodes and/or neural crest cells (NCCs). The bilateral retinas arise from the optic field, located on the midline of the neural plate, that will separate as the neural tube forms, generating the optic vesicles (Cavodeassi *et al.*, 2013; Ivanovitch *et al.*, 2013; Varga *et al.*, 1999). Concurrently the progenitor fields giving rise to the olfactory placode (OP) and olfactory bulb (OB/Tel) converge anteriorly passing dorsal to the forming optic stalk region (Torres-Paz and Whitlock, 2014). Thus the morphogenesis of the visual system and the OP/OB occur at the same developmental time window, initiated at the end of gastrulation, and form through carefully orchestrated cell movements within the neurectoderm.

The cranial nerves, responsible for the efferent and afferent connections between the PNS/CNS, are paired nerves where ten of the twelve pairs (III-XII) either target or initiate from the brainstem (Angeles Fernandez-Gil *et al.*, 2010). Cranial nerves I (olfactory nerve) and II (optic nerve) are distinct: not only do they not join with the brainstem, they also have a continuous meningeal covering (O'Rahilly and Muller, 1986). Thus the structure of the olfactory nerve is similar to the optic nerve. In the olfactory system, the fila, or bundles of the olfactory nerves pass through the cribriform plate surrounded by a meningeal covering (arachnoid) (Favre *et al.*, 1995; Levine and Marcillo, 2008; Walker, 1990). The meninges (pia, arachnoid and, dura mater) surround the olfactory nerves creating a subarachnoid space that extends through the cribriform plate into the nasal mucosa containing the large blood vessels that supply olfactory epithelium (Galeano *et al.*, 2018). This meningeal organization is shared only with the optic nerve and suggests that not only the visual sensory epithelia (retina) but also the OE may form from the neural plate as opposed to secondarily induced placodes

At the anterior edge of the neural plate combinatorial expression of genes belonging to the families SIX (sine oculis), EYA (eyes absent) and DLX (distal-less), are expressed the different placodal domains with a particular molecular signature (Schlosser and Ahrens, 2004) (Schlosser, 2010). Previously it has been shown in fish and amphibians that at the end of gastrulation there are distinct levels of *dlx3* expression across the anterior neural plate with higher levels at the edge, and lower levels medially.(Akimenko *et al.*, 1994; Franco *et al.*, 2001; Whitlock and Westerfield, 2000). Fate mapping analysis has shown that the high-expression domain will give rise to OE cell types and the low-expression domain to olfactory bulb cell types (Whitlock, 2004; Whitlock and Westerfield, 2000). The physical separation of the future OE and OB occurs progressively with the formation of a basal lamina at early somitogenesis, followed by anterior migration of the cranial NCCs, resulting in the OPs becoming morphologically evident at 18 somite stage of development (Harden *et al.*, 2012; Torres-Paz and Whitlock, 2014).

Here we test the hypothesis that the distinct levels of Dlx3b/4b expression are instructive for conveying identity of peripheral and central olfactory system precursors by manipulating levels of Dlx protein during early somitogenesis stages. Through analysis of low-density cell clones, we observed that some cells maintain connections across the morphological divide of the future OE and OB suggesting cellular continuity within the neurectoderm well before the physical appearance of these structures. Consistent with our hypothesis, in some cases the reduction or over-expression of DLX proteins resulted in changes in the relative sizes of the olfactory placode-olfactory bulb/telencephalon regions. Thus our results support a role for Dlx3b/4b in regulating a balance between OE and OB precursors at the progenitor levels ensuring the proper segregation cells during olfactory field separation. Taken together, our data suggest that the olfactory system develops as a functional unit, where the peripheral sensory epithelium (the source) and the OB (the central target) develop in tandem, instead of as separate pieces that integrate once formed (Whitlock, 2008, 2015).

Results

Cell organization within the developing olfactory epithelium

By comparing the expression of different transgenic reporter lines and antibodies recognizing proteins in the developing OPs we found a heterogeneous composition of precursor cells before placode becomes morphologically obvious at 18-20 somite stage (ss, Whitlock and Westerfield, 2000). As previously described, Dlx3b expression is observed during development of the olfactory system, with high levels in the OP precursors and lower levels towards the midline, where the precursors of the OB are located (Fig. 1A, B, (Torres-Paz and Whitlock, 2014; Whitlock and Westerfield, 2000). Previously we generated the *six4b:mCherry* transgenic line as a marker for the developing OP (Harden *et al.*, 2012) where it is expressed throughout life in putative support cells in the OE. At 14ss (Fig. 1C arrows), cells at the more anterior region of the OP domain in the forming neural tube are positive for both Dlx3b antibody (Fig. 1, C, C'', green, arrow) and Six4b:Cherry (Fig. 1C, C', red, arrow). In contrast, cells at the more posterior region of the OP domain in the forming neural tube are positive for only Dlx3b antibody (Fig. 1, C, C'', green, arrowhead). The subset of cells expressing Six4b:mCherry (Fig. 1C, C', red, arrow) and Dlx3b antibody (Fig. 1, C, C'', green, arrowhead) suggests that Dlx3b+
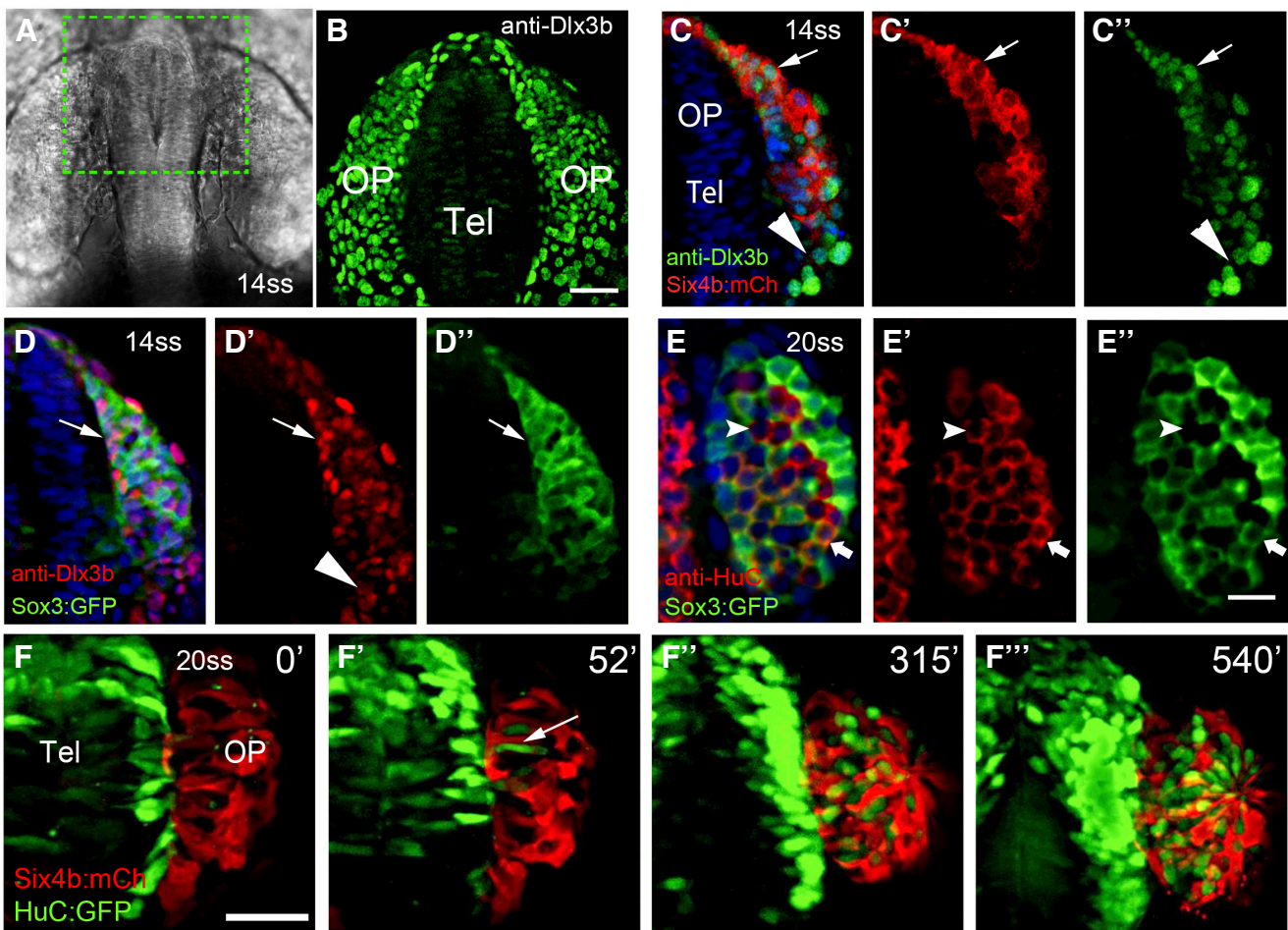
Fig. 1. Cell organization during olfactory epithelium (OE) development. (A) *Green dotted outlined indicates the region shown in B.* **(B)** *Dlx3b expression in prospective OP and telencephalon (Tel).* **(C-C")** *Double labeling for anti-Dlx3b (C,C", green) and Six4b:mCherry (C,C', red) in the forming OP with double labeled cells indicated (arrow) and cells positive for only Dlx3b (arrowhead).* **(D-D")** *Double labeling of anti-Dlx3b (D, D', red) and Sox3:GFP (D, D", green) with double labeled cells indicated (arrow).* **(E-E")** *Double labeling antibody recognizing HuC (E, E', red) and Sox3:GFP (E, E", green) in the OP. Arrows indicate double labeled cell, arrowheads cell positive for only HuC.* **(F-F''')** *Images from a 9 hour time lapse movie of a double transgenic embryo six4b:mCherry (red) and HuC:GFP (green) showing one OP. F' arrow indicate appearance of neurons in OP. (A,B,C,D) Dorsal view of head at 14 ss, anterior to the top of the page; (E,F) frontal view at 20 ss. (B) A projection of 20 µm; (C,D,E) 3 µm; (F) 10 µm. (F) Frontal view, dorsal upwards. Scale bars: B, 25 µm; C,D,E, 20 µm; F, 25 µm.*

cells can differentiate into Six4b:mCherry+ support cells consistent with their classification as potential multipotent progenitor cells. To further investigate the identity of Dlx3b positive cells as precursor cells, we used the *sox3:GFP* line. This line does not recapitulate the total expression pattern of the *sox3* gene in zebrafish, where this gene is expressed in the neural plate at the end of gastrulation (Dee *et al.*, 2008). Important for our experiments, the line has a well described expression pattern OP precursors (*Sox3:GFP;* Navratilova *et al.*, 2009). Similar to Six4b:mCherry positive cells (Fig. 1C, red), the Sox3:GFP+ cells (Fig. 1D, D", green, arrow) co-localized with anti-Dlx3b+ cells anterior region of the OP domain in the forming neural tube (Fig. 1D, D', red, arrow), but there was no co-localization in the posterior region of the OP domain in the forming neural tube (Fig. 1D, D', red, arrowhead). This labeling pattern is consistent with Dlx3b expressing cells being multipotent progenitors cell capable of generating support cells and neurons. Using an antibody recognizing HuC, a general marker of new-born neurons, in the *sox3:GFP* line we found that subset of the anti-HuC

positive neurons (Fig. 1E, E', red arrow) at 20 ss were also positive for Sox3:GFP+ (Fig. 1E, E" green, arrow) where as other anti-HuC positive cells (red) did not co-label for Sox3:GFP (Fig. 2E, E', E", arrowhead). The dynamics of neurogenesis were examined using embryos doubly transgenic for *six4b:mCherry;HuC:GFP* to mark the OP (Fig. 1F-F'", Supplemental movie 1; red) and new neurons (Fig. 1F-F'", Supplemental movie 1; green). At 20ss neurons are already present in the developing telencephalon (Fig. 1F, green). HuC:GFP expression appears later in the OP (Fig. 1F', green, arrow) in the first differentiating neurons. As new neurons were added we never observed cells co-expressing HuC:GFP and Six4b:mCherry (Fig. 1F", 1F'"), consistent with the expression of Six4b:mCherry in support cells, to date the only marker for this lineage in zebrafish. Together these data suggest that from the end of gastrulation onward Dlx3 is expressed in multipotent OP precursors (Sox3:GFP positive), and at 14ss, before OPs are apparent, there are already indications of lineage restrictions to neuronal (HuC-positive) and non-neuronal (support cells, Six4b:mCherry) lineages.

Clones of cells maintain contact across morphogenetic fields

To test the model of a continuous neurectoderm generating the OB and OP, we analyzed individual cell movements and morphology at stages when OPs are developing. Representative images of random mosaics of cells expressing a membrane-targeted GFP in the region of the OP/OB (Fig. 2, green, n_{total}l = 8) were generated by injection of a cDNA construct encoding for *Gap43-GFP*. We performed co-labeling with anti-laminin antibody (Fig. 2, red) to observe the forming boundary between OB and OP (see (Torres-Paz and Whitlock, 2014)). Embryos with low density cell clones were analyzed where the initial image (Fig. 2, A, B, C, D) was deconvoluted (Fig. 2, A1, B1, C1, D1) and an optical section of three microns (Fig. 2, A2, B2, C2, D2, boxed areas) was analyzed at higher magnification with separate red (Fig. 2, a2, b2, c2, d2) and green channels (Fig. 2, a2', b2', c2', d2') for each group of cells. Before OP formation at 12 ss (Fig. 2A, B) and after OP formation at 20ss (Fig. 2, C, D) clones of cells in the developing placodes and/or telencephalon were analyzed. Because the GFP is targeted to the membrane the outlines of cells can be visualized to determine whether they maintain contact across the developing laminin border. At 12 ss, we observed clones with (green) extensions that appeared to cross the forming basal lamina (Fig. 2, A2, a2, red, arrow) that will eventually separate the OP from the OB/Tel (Torres-Paz and Whitlock, 2014). We also observed clones that appeared to cross the laminin border but in optical sections the contact did not appear to be continuous (Fig. 2, B2, b2, b2', arrowheads). Some cells in the OP appeared to maintain contact with potential sister cells in the telencephalon when scored after the morphological differentiation of the OPs at 16-18 ss (Fig. 2, C1, D1, boxed areas). At 20ss one clone (Fig. 2, C1) had GFP+ processes extending across the laminin border (Fig. 2 C2, c2', arrows). The morphology and location of the cell body in the OP (Fig. 2 C2, arrowhead, c2', arrow) is reminiscent of previously described pioneer neurons in the olfactory placode (Whitlock and Westerfield, 1998), a class of transient neurons proposed to guide and coordinate the development of the olfactory sensory neurons. In contrast to the cells seen in Fig. 2 C, in Fig. 2 D the cells in the OP are elongated, and also send a process across the laminin border (Fig. 2 D2, d2', green). At this developmental stage the laminin border is further elaborated to form the previously described lamina associated with the OP (Fig. 2, d2, asterisk) and with the neural tube (Fig. 2 d2, double asterisk). A preparation containing groups of cells at higher density, thus not suitable for clonal analysis, showed tightly associated groups of GFP positive cells in the OP and adjoining telencephalon (Supplemental movie 2). Although the Gap43-GFP labeling is not a lineage tracer *per se*, clusters of cells at low densities can be assumed to share a progenitor or limited number of progenitors.
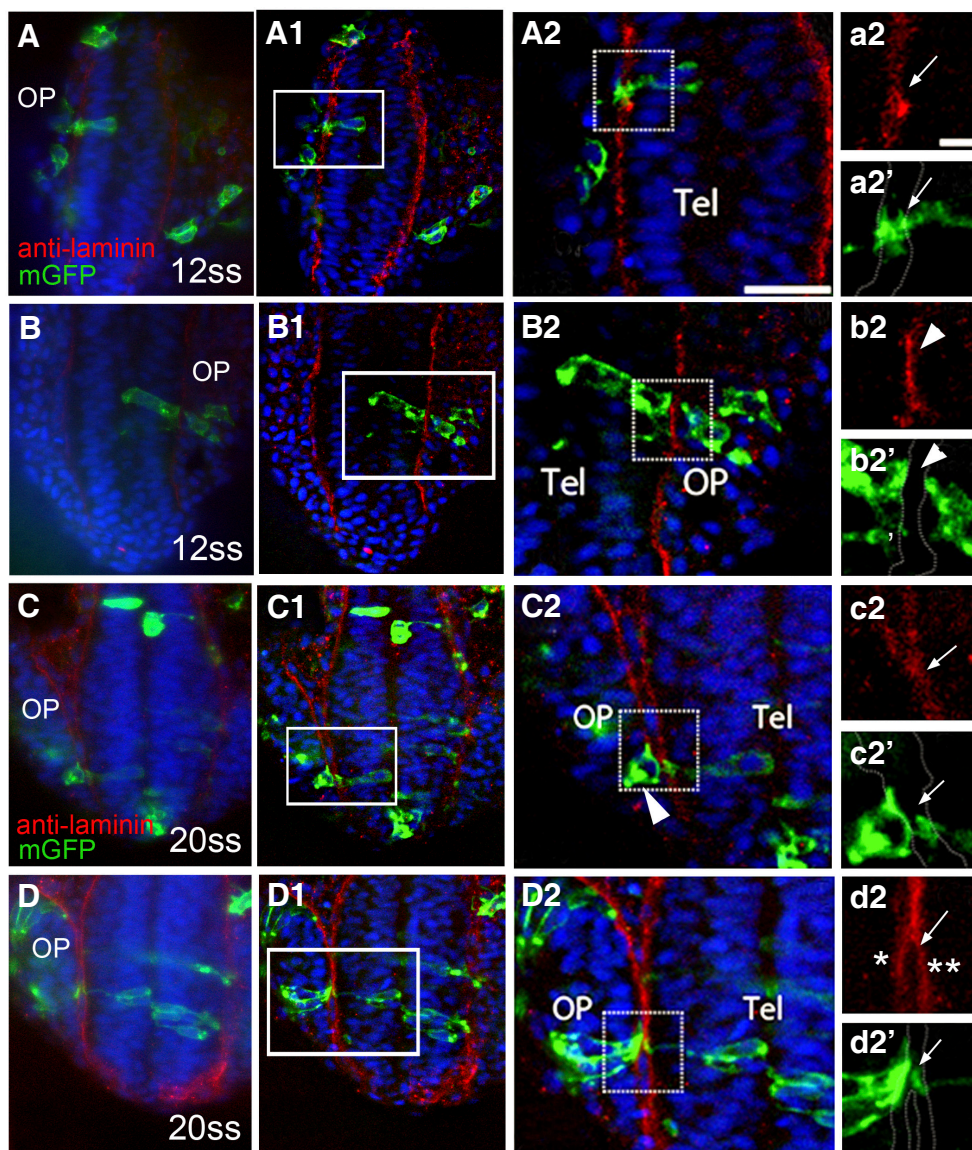
Fig. 2. Low density clones in the developing olfactory system suggest shared progenitors. (A-D) *Representative images of mosaic Gap43-GFP expression (green, cell membrane) and laminin staining (red) at the border between developing OP and telencephalon (Tel).* **(A-D)** *Low magnification images of the head region of fixed embryos at 12ss (A, B, n=5) and 20ss (C, D, n=3).* **(A1-D1)** *Same images as (A-D) but processed by deconvolution. Boxed areas indicate groups of cells analyzed.* **(A2, B2, C2, D2)** *Cells (boxed areas) with connections joining the OP and Tel region at 12 somites (A2) and 20ss (C2, D). Insets of boxed area where cells (**a2', c2', d2'**; green) maintain connections across the laminin positive border (**a2, c2, d2,** red). **(B2, b2)** Insets of boxed area showing cells (b2', green) appear to lose connections at the laminin border (b2, red). **(C2)** Cell observed in OP (arrowhead) has characteristic of pioneer neuron and maintains connections across the laminin positive border (c2, c2'). Dotted lines A", B", C", D" represent the basal lamina. Scale bar: A, B, C, D, 50 µm; insets, 10 µm.*

The specific identities of these cells are unknown, yet the clones reflect an intimate association of the progenitors in the neurectoderm before the formation of the neural tube. These results support a model where the OPs and OBs arise from a continuous sheet of neurectoderm with the potential that some lineages generate progeny in both the OP and OB.

Decrease in DLX results in reduced olfactory placode field

To test our model that distinct levels Dlx are instructive cue for the formation of the OPs (high DLX) versus OB/Tel (low DLX) we used morpholino technologies to decrease DLX protein expression in the developing neural plate. Most DLX genes are grouped in pairs sharing regulatory sequences, thus having overlapping expression patterns with redundant functions (Quint *et al.*, 2000; Zerucha *et al.*, 2000). In zebrafish the linked pair *dlx3b* and *dlx4b* (*dlx3b/4b*) are important for the development of olfactory and otic placodes. Specifically we targeted the protein products of *dlx3b/4b* during olfactory morphogenesis using a knockdown approach known to generate a highly specific phenotype (Esterberg and Fritz, 2009; Solomon and Fritz, 2002; Solomon *et al.*, 2004); see Fig. 4 below).

To assay the effects of decreased DLX proteins on the OP-OB/Tel fields, *dlx3b/4b* MO knockdowns were performed in *six4b:mCherry*/*sox3:GFP* double transgenic embryos utilizing the expression of both reporters to measure OP volume (Fig. 3). At 24 hpf morphant embryos showed a significant reduction in the size of the OP (Fig. 3 B, E; red, S+S, Six4b:mCherry + Sox3:GFP) compared to embryos injected with the control *M*Os (Fig. 3, A, E; blue, S+O, Six4b:mCherry + Sox3:GFP). Ectopic expression of Sox3:GFP was observed in the region of the OB/Tel in the morphants (Fig. 3B, asterisks), The GFP expression observed in the OB/Tel is transient, disappearing after 48 hpf. We interpret this result as the perdurance of the GFP protein initiated in the OP precursors before morphological border formation. Cells expressing low Dlx3b levels (*dlx3b/4b* MO) would end up in the telencephalon, and later, GFP would be down-regulated. In contrast, we never observed ectopic mCherry expressing cells, suggesting that Sixb:mCherry expression in OP is limited to differentiated cell types.

To determine whether the reduction in OP size observed in *dlx3b/4b* MO was maintained at later stages of olfactory organ development, 5 day post-fertilization (dpf) *omp:YFP*; *six4b:mCherry* larvae were used to visualize both the ciliated OSNs (Fig. 3, C, D, green) and support cells (Fig. 3, C, D, red). A marked reduction in size in the developing olfactory organ (OO) is maintained even after 5 dpf in the morphant embryos (Fig. 3, D, E; red, S+O, Six4b:mCherry + OMP:YFP) compared to the control embryos (Fig. 3; blue S+O, Six4b:mCherry + OMP:YFP). Although the OO is significantly smaller in the morphants, OSN axons terminate in stereotypic glomerular patterns in the OB (Fig. 3C, D, arrows). Additionally, we found that *six4b:mCherry* labels some facial neuromasts close to the OO, which are unaffected in the *dlx3b/4b* morphant embryos (Fig. 3, C, D, arrowheads). Normally Dlx3b expression decreases after 24 hpf (Torres-Paz and Whitlock, 2014), thus a reduction in Dlx3b protein levels during early development leads to smaller olfactory organ a five dpf (MOs are functional until

about five days post fertilization), potentially by limiting the pool of progenitors. This shift in precursor allotment is consistent with the initiation of *dlx* expression the end of gastrulation thus defining precursors within the continuous neural plate that will further segregate into the peripheral and central olfactory system based on levels of DLX.

Potential role of proliferation and cell death in reduced olfactory placode size

To determine whether the observed changes in OP were due to an alteration in mitotic rates, we analyzed the number of cells positive for the mitotic marker phosphorylated histone (PH3) in the OPs. On average we found fewer positive cells in the placodes of
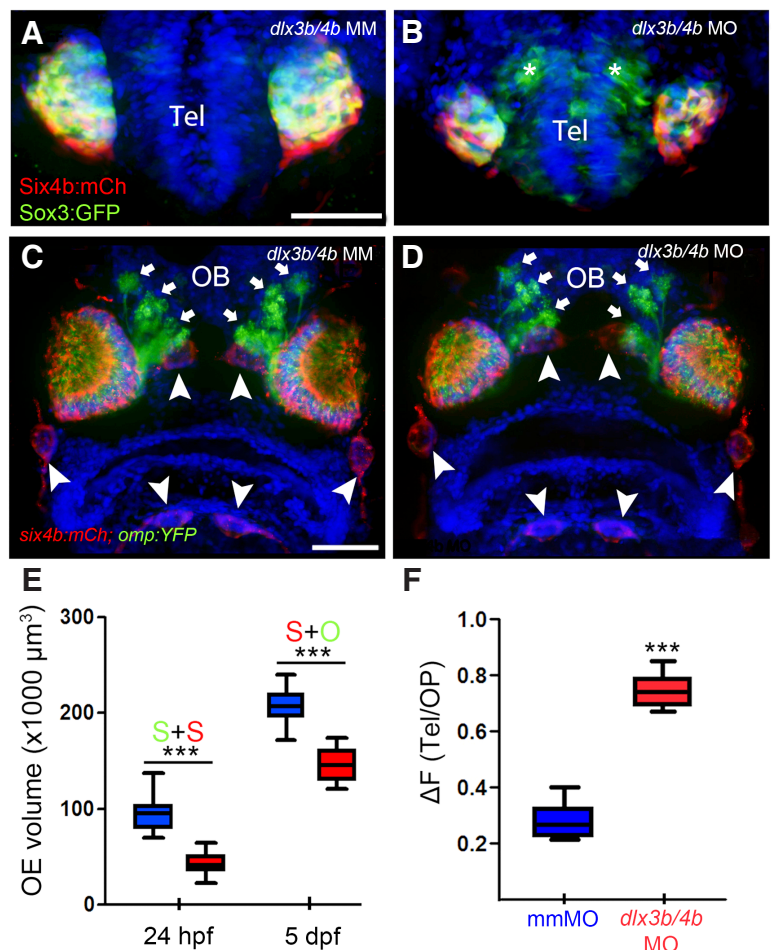
Fig. 3. Decrease in Dlx3b/4b protein reduces olfactory placode size. (A,B) *Representative preparations of Sox3:GFP (green) and Six4b:mCherry (red) expression in embryos at 24 dpf in the OPs of dlx3b/4b MM (A, n=12) and dlx3b/4b MO injected embryos (B, n=12). Asterisks indicate ectopic expression of GFP in the developing telencephalon. **(C,D)** 5 dpf six4b:mCherry (red) OMP:YFP (green) expression in larvae injected with control mmMO (C, n=19) and dlx3b/4b MOs (D, n=16). Arrows indicate olfactory nerve endings in glomerular layer of the OB. Arrowheads indicate facial neuromasts. **(E)** Graph representing the volumes of OE measured in dlx3b/4b MM (blue), dlx3b/4b MO (red) injected embryos at 24hpf (S+S, Sox3:GFP + Six4b:mCherry) and at 5 dpf (S+O, Six4b:mCherry + OMP:YFP). **(F)** Graph representing the ratio of GFP fluorescence intensity (telencephalon/OP) in dlx3b/4b MM (blue) and dlx3b/4b MO (red) injected embryos. Images A and B are dorsal views; C-F are frontal views. Scale bars, 50 µm.*
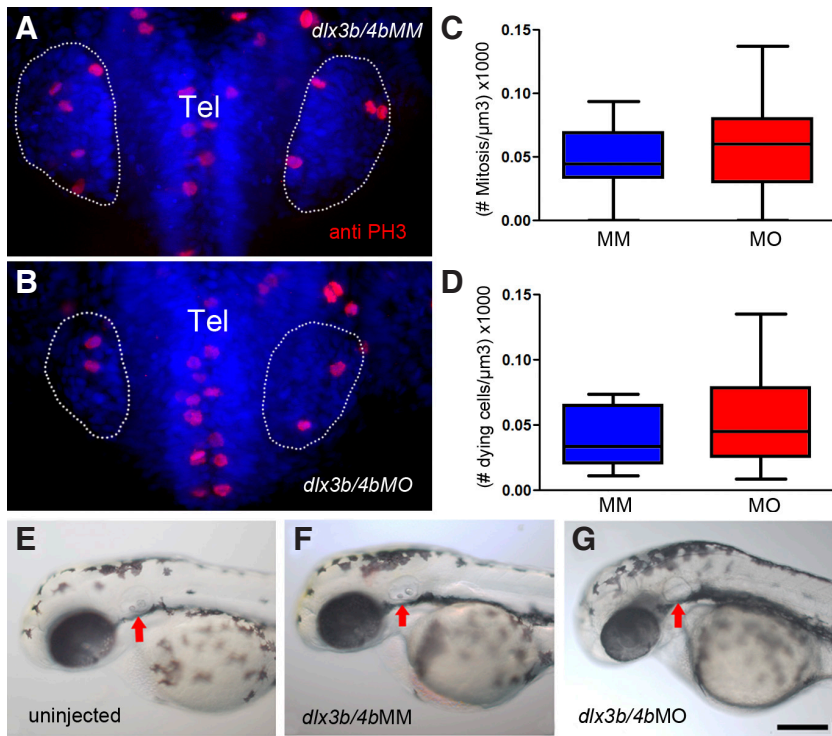
Fig. 4. Reduction in olfactory placode (OP) size in Dlx3b/4b deficient embryos is not due to changes in the rate of cell division or cell death. (A,B) *Mitotic cells (PH3+ cells, red) in the OP (dashed line circles) and developing telencephalon in control mmMO (A) and dlx3b/4b MO injected embryos (B).* **(C)** *Quantification of mitotic cells in OPs normalized in the volume measured ($\mu m^3/10^5$) in control (blue, n = 11) and dlx3b/4b morphant embryos (red, n=12).* **(D)** *Quantification of Acridine orange labeled cells in the OPs normalized in the volume measured ($\mu m^3/10^5$) in dlx3b/4bMM control (blue, n = 11) and dlx3b/4bMO morphant embryos (red, n=12). Scale bar, 50 μm. n = 12 for each condition. Images are frontal views.* **(E-G)** *Phenocopy of morphant otic phenotypes in dlx3b/4bMO injected embryos. Uninjected embryo (E), dlx3b/4bMM (F) and dlx3b/4bMO injected embryos (G) after 45 hpf. Red arrows indicate the otic vesicle. Note the absence of the otoliths (two dots inside the vesicle) in the morphant embryo. lateral views, anterior to the left. Scale bar, 100 μm.*
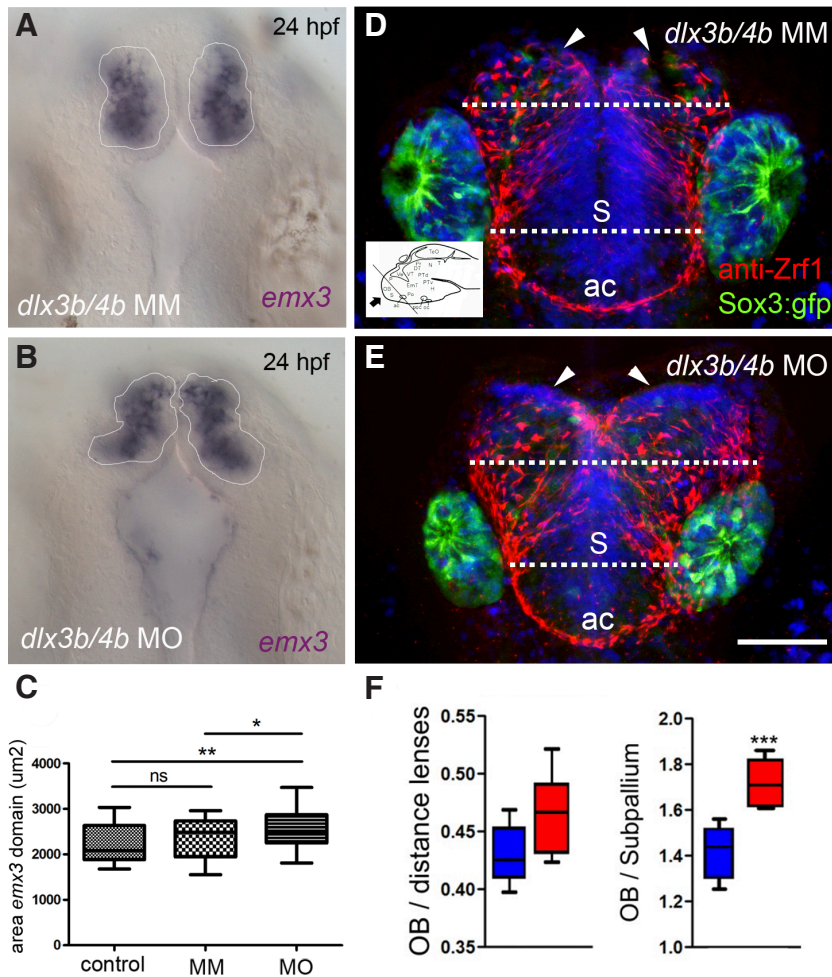
Fig. 5. Reduction in distal-less (DLX) proteins expands the olfactory bulb (OB) domain as assayed by *emx3* transcription factor. (A,B) emx3 *expression in the developing telencephalon (purple, arrowheads) of control dlx3b/4b MM (A, n=16) and dlx3b/4b MO injected embryos (B, n=34) at 24hpf.* **(C)** *Quantification of area expressing* emx3 *at 24 hpf. Statistically significant differences in* emx3 *expression (area) between uninjected controls (n=15) and dlx3b/4b morphants (n=34) (p-value = 0.0015, **), between MM controls (n=16) and dlx3b/4b morphants, (p-value = 0.0143, *). No differences were observed between uninjected controls and dlx3b/4b MM controls, (p value = 0.5572, ns). Two-tailed test.* **(D,E)** *Anti-Zrf1 labeling (red) in radial glia of the CNS in control dlx3b/4b MM (D) and dlx3b/4b morphant (E) injected sox3:GFP (green) embryos at 2 dpf. Morphant animals showed everted telencephalic phenotype (E, arrowheads) relative to the MM controls (D, arrowheads). Upper white dashed lines indicate the borders in the developing OB where widths were measured. D inset: zebrafish brain at 2 dpf, lateral view, anterior to the left and dorsal up, oblique line indicates the level of optical section.* **(F)** *The ratio of OB width/distance between lenses of the eye in dlx3b/4b MM (blue) and dlx3b/4b MO (red) animals (left, p value = 0.0525, n=10 scored). Scale bar (A-D) 50 μm. (A,B) are dorsal views; (C,D) are frontal oblique (arrow in D, inset). ac, anterior commissure; OB, olfactory bulb; S, subpallium. Inset in (D) adapted from Mueller and Wullimann, 2005).*

morphant embryos (2.1~1.7, average ~ SD; Fig. 4) compared to the controls (5.2~2.6, average+/-SD; Fig. 4). However, this reduced number could be due to a proportional decreased in the size of placodes in the morphants. To further analyze whether the differences were due to changes in tissue proliferation, we normalized the number of cells positive for mitosis marker by the volume of the placode, and we found no statistically significant differences (Fig. 4C). It has been described before that cell death pathways are particularly activated in response to MOs injections (Robu *et al.*, 2007). To determine whether the reduced size of the OP was due to cell death, *dlx3b/4b* MM and *dlx3b/4b* MO injected embryos were labeled with Acridine Orange (AO) that marks cells undergoing cell death. The AO labeling did not show global increases in cell death relative to the controls (Fig. 4). These results support the conclusion that the reduction in volume of the OPs in the morphants is not due to a reduction in the rate of cell divisions or increase apoptotic mechanisms, but rather results from DLX protein induced shift in the specification to OB/Tel fate before the separation of both tissues.

Our *dlx3b/4b* morphants are a phenocopy of the previously reported highly specific, phenotype (Solomon and Fritz, 2002; Solomon *et al.*, 2004) (Esterberg and Fritz, 2009). In agreement with previous descriptions, we observed a lack of otoliths in *dlx3b/4b* morphants, whereas embryos injected with the *dlx3b/4b* MM control looked similar to uninjected control (Fig. 4, E-G, red, arrows). In addition to the otic phenotype, larval morphology, including head size, was normal, highlighting the specificity of this treatment.

Dlx3b depletion affects telencephalon development

During development the expression of Dlx3b is high in OP precursors and lower in the adjacent OB/Tel precursors thus we

generated *dlx3b/4b* morphant embryos *to* determine whether decreases in DLX protein expanded OB precursor domains. We analyzed through *in situ* hybridization the expression of *emx3*, a well-known marker of the dorsal telencephalon, including the developing OB, in vertebrates (Kawahara and Dawid, 2002; Sen *et al.*, 2013). The general pattern of *emx3* expression at 24 hpf was conserved in *dlx3b/4b* MM *c*ontrol embryos (Fig. 5, A, outlined area) and *dlx3b/4b* morphants (Fig. 5, B, outlined area). We quantified the area of *emx3* expression in uninjected control (n=15), MM control (n=16), and morphant (n=34), embryos at 24 hpf (Fig. 5C). Statistically significant differences were observed in the area of *emx3* expression between uninjected controls and *dlx3b/4b* morphants (Fig. 5, C, p-value = 0.0015, **) as well as between MM controls and *dlx3b/4b* morphant (Fig. 5, C, p-value = 0.0143, *) while no differences were observed between uninjected controls and MM controls (Fig. 5, C, p value = 0.5572, ns).

To further analyze the development of the OB/Tel at 2 dpf (days post-fertilization) we used the anti-ZRF1 antibody, a general marker of radial glial cells (Trevarrow *et al.*, 1990) that is expressed in the developing telencephalon (Fig. 5, D, E). The width of the developing OB/Tel was measured and normalized by the distance between lenses where there was an increase, although not significant (p value = 0.0525), in the value obtained in the morphants (Fig. 5, F, red) compared to embryos injected with the control *dlx3b/4b* MM *(*Fig. 5, F, blue). A phenotype evident in *dlx3b/4b* morphants at both 24 hpf (Fig. 5B) and 2 dpf was that the pallium was altered such that it "splayed" outward (Fig. 5, E, arrowheads). Initially we normalized the width of the developing OB/Tel to the width of the subpallium in *dlx3b/4b* MM *(*Fig. 5, D, S) and *dlx3b/4b* morphants (Fig. 5, E, S). Yet upon closer analysis the subpallium is reduced in size relative to the MM controls. While Dlx3/4 and their orthologues

Fig. 6. Reduction in DLX proteins expands OB population of periglomerular interneurons. *(A,B)* *Anti-Tyrosine Hydroxylase (TH) labeling in periglomerular neurons of the OB (red) in 3 dpf* omp:YFP *larvae. Images are from the same animal at a focal plane (A), where axons of the olfactory nerve arrive (A', green, arrowheads) contacting TH neuropil (A'', red, arrowheads), and at a deeper focal plane* **(B)***, where there are no OSN axons (B') and TH cell bodies are still present (B'', red, arrows).* **(C,D)** *Representative images (15 µm projections) of anti-TH labeling in the OB (red) in 3 dpf embryos injected with control dlx3b/4b MM (C, n = 14) and dlx3b/4b MO (B, n = 13).* **(E)** *Number of TH neurons are significantly greater in dlx3b/4b MO (red) compare to dlx3b/4b MM injected embryos (blue, p = 0.0025, Mann-Whitney). Scale bar = 50 µm.*
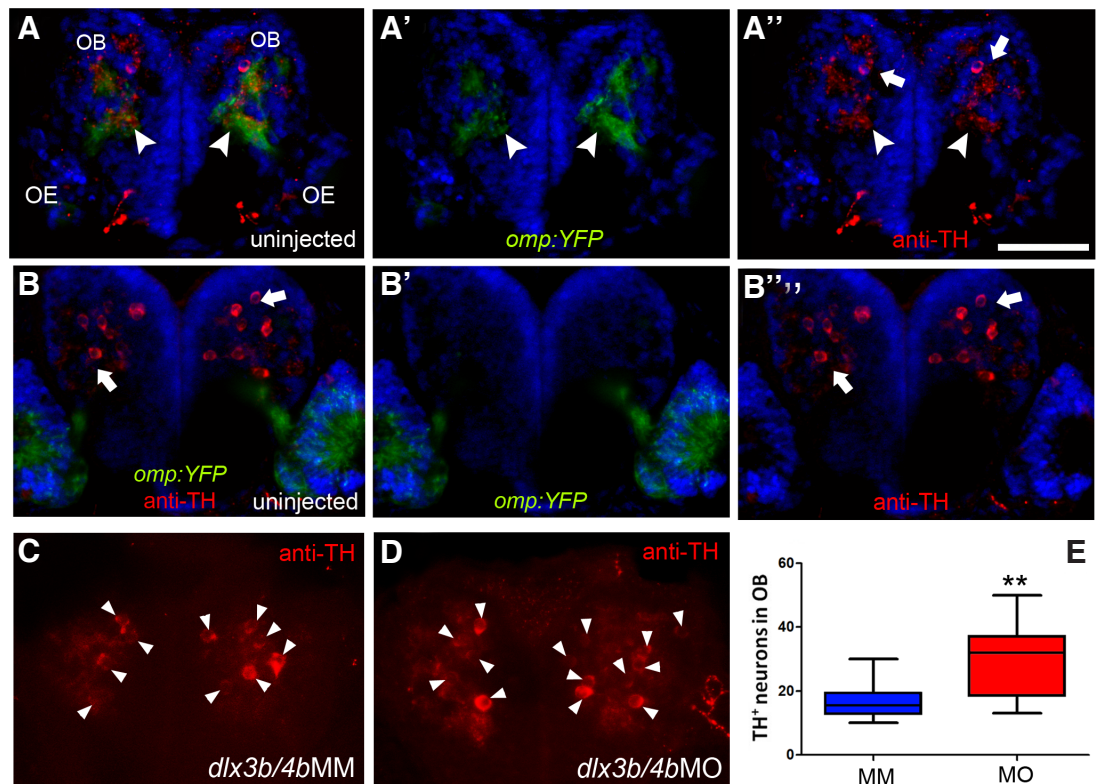
are not reported to be expressed in the subpallium (MacDonald *et al.*, 2010), the reduced size evident in Fig. 5E suggests that the enlargement of the OB/Tel (part of the pallium) may come at the expense of not only the re-allocation of OP progenitors, but progenitors of the subpallium. The reduced levels of Dlx3b/4b proteins result in not only changes in the OPs but also concomitant morphological changes in the developing OB (considered part of the pallium)/Tel, and potentially the subpallium, thus suggesting that during development the peripheral and central olfactory sensory system are intrinsically linked precursor fields.

### Reduced olfactory placode fields result in increase of olfactory bulb interneuron types

Because the reduction of DLX results in the expansion of OB, to determine potential effect on differentiated sensory neurons in the OB we used an antibody recognizing tyrosine hydroxylase (TH), the rate-limiting enzyme in catecholamine biosynthesis, and a marker of dopaminergic periglomerular neurons in the OB (Holzschuh *et al.*, 2001). We performed immunofluorescence to detect TH expression in *omp:YFP* transgenic larvae at 3 dpf, in order to visualize periglomerular neurons and axonal efferent from the ciliated OSNs at the same time (Fig. 6, A, B). We observed that in the superficial layer of the larval OB (Fig. 6, A-A"), the signal corresponding to the end of the olfactory nerve arriving to the glomeruli (Fig. 6A', arrowheads) coincides with TH immunoreactivity, possibly corresponding to dendritic neuropil. In this optical section some cell bodies can also be observed (Fig. 6, A', arrows), although most of the periglomerular somas are located at deeper sections of the OB (Fig. 6, B, B"). We next analyzed the number of anti-TH positive neurons in the developing OB of *dlx3b/4b* control and morphant embryos. To quantify the number of TH positive cells we generated projections of the olfactory bulb region that encompassed the limits of TH+ cell population and all identified TH+ cell bodies were counted in the acquired Z-stack (Fig.

6, C, D, arrows). On average there were 8.8 TH+ cells in *dlx3b/4b* MM and 17 TH+ cells in *dlx3b/4b*MO animals when scored at 3 dpf, thus a significant increase (p = 0.0028) in the number of TH positive neurons (Fig. 6, D, E) compared to control embryos (Fig. 6, C, E). Together, our data suggest that decreased Dlx3b activity results not only in an expansion of OB/Tel precursors (*emx3*) but an increase in the number of OB interneurons.

Increase in DLX results in expanded olfactory placode field

To test whether an over-expression of *dlx3b* would increase the size of the OP potentially at the expense of the OB, we over-expressed *dlx3b* by mRNA injection (Esterberg and Fritz, 2009) in embryos just after fertilization (Fig. 7). Because the expansion of the OPs may come at the expense of the OB/Tel precursors, *in situ* hybridization using probes for the transcription factors *emx3* and *emx1* known markers of OB/Tel precursors, were performed in embryos to determine whether there was a reduction in expression at 24hpf. For the *emx3* (Fig. 7, A, B) and *emx1* (Fig. 7, C, D) expression domains in the telencephalon, there was no significant difference (Fig. 7, E, F). As was noted previously (Fig. 5) in *dlx3b/4b* morphants the ventricle (Fig. 7, C, D, v) was expanded outward making projections difficult to normalize between control and experimental groups.

Expression of *emx1* and *emx3* was also observed in the OPs, (Fig. 7, A-D, dashed circles), however quantification of positive cells was not possible because the expression domains were dynamic: the number and location of *emx1* and *emx3* expressing cells (Fig. 7, A-D, arrows) was too variable. Thus we allowed *omp:RFP;sox3:GFP* embryos injected with mRNA of *dlx3b* to develop until 5 dpf and the volume of the OP (Fig. 7 G, H, arrows) was scored. A small but significant increase in the size of the OE was observed (p = 0.0209). In general the experiments where we over-expressed *dlx3* mRNA were limited by the fact that the developing embryos were negatively affected at all concentrations
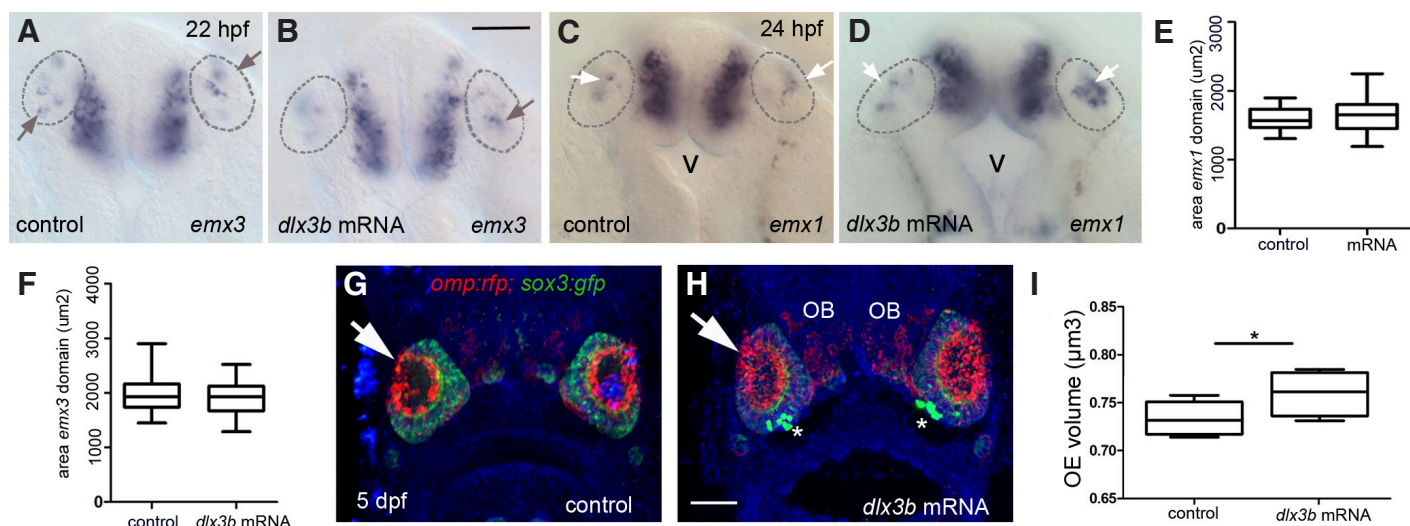
Fig. 7. Over expression of distal-less (DLX) affects olfactory placode (OP) development. *Expression of* emx3 *at 22 hpf* **(A,B)** *and* emx1 *at 24hpf* **(C,D)** *in uninjected control embryos and* dlx3b mRNA *injected embryos. Quantification of areas expressing* emx1 **(E)** *and* emx3 **(F)** *in the OB/Tel. No statistically significant differences in* emx3 **(A,C,F)** *or* emx1 **(B,D,E)** *expression were between uninjected controls and* dlx3b mRNA *although quantification was difficult expanded ventricle. No quantification was made of the expression pattern (arrows) in OPs (dashed circles) due to high individual variability in the number of cells labelled.* **(G,H)** omp;RFP; sox3:GFP *larvae at 5 dpf where* dlx3b mRNA *injected animals show small increases the size of the olfactory organs (arrows). Asterisks in H are Gnrh3;GFP cells that are in our* omp:rfp *line.* **(I)** *Injection of* dlx3b mRNA *results in small but significant increase in the size of OOs (p = 0.0209). (A-D) Dorsal views; (G,H) frontal views. Scale bars: (A-D) 40 μm; (G,H) 50 μm.*

of the injected mRNA showing high lethality. Perhaps due to the genetic redundancy of *dlx* genes in zebrafish, reduction in protein levels is better tolerated than over expression of proteins. The limited over-expression data suggest that the over-expression of the *dlx3b* may affect the size of the OP although more analyses are needed with different markers.

Discussion

Early development is characterized morphological movements that are highly conserved across species: gastrulation generates the endodermal, mesodermal and ectodermal germ layers, with the subsequent induction of the neurectoderm from the overlying ectoderrm. At the end of gastrulation segmentation is initiated, and the complex cell movements lead to the formation of the neural tube and associated placodal structures. The classic view on how placodal structures develop is based on studies in the visual system showing that the lens, a non-neural tissue, is induced from the over-lying ectoderm by the optic vesicles. This model for sensory system development was then applied ubiquitously to the peripheral sensory systems regardless of the cell types generated. Previously we have shown that the field of neurectoderm giving rise to both the olfactory bulb and olfactory placode are continuous consistent with the first fate map studies of the olfactory placode in zebrafish (Torres-Paz and Whitlock, 2014; Whitlock and Westerfield, 2000). Here we have tested the hypothesis that *dlx3b/4b* genes play a role in delineating the peripheral from the central neurons through distinct levels of protein expression established at the end of gastrulation. By characterizing markers expressed in the developing olfactory system as well as analysis of clones and expression studies, we find that, consistent with our model, the early precursor field giving rise to the peripheral and central olfactory system is continuous. Furthermore through the reduction or over-expression of DLX proteins we were able to affect the relative sizes of the olfactory placode and olfactory bulb/telecephalon regions thus supporting the role of DLX3 in the division of the precursor field without obvious changes in general organization.

Are all placodes the same?
During evolutionary time sensory systems were elaborated to different degrees in different groups of chordates in response to selective pressures. Sensory modalities did not all arise at the same time, thus supporting a potentially non-uniform development and function of sensory systems in modern vertebrates where there are substantial differences between placodes in terms of early development, organogenesis and integration in the nervous system. For example, recent studies examining adenohypopyseal placode development have shown an early cellular and molecular heterogeneity where the cellular morphology and gene expression patterns are distinct from that of the flanking "pre-placode" domain, (Sanchez-Arrones *et al.*, 2017). Furthermore the adenohypophyseal placode may share common cellular and molecular characteristics with the developing pineal organ another neuroendocrine derivative of the lateral border of the anterior neural plate (Staudt *et al.*, 2019). Thus the tendency to group sensory placodes as a bunch of coherent structures may be misleading as each sensory placode has very different characteristics (Begbie *et al.*, 2002; Begbie and Graham, 2001). The olfactory placode is unique because it contains group of sensory neurons that are replaced throughout life and

these sensory neurons send their axonal projections to the OB. Like the olfactory sensory epithelium, the retina of the eye contains retinal ganglion cells, projection neurons that extend axons to their central target in the midbrain. This is in direct contrast to taste and hearing where the (placodally derived) sensory receptors are innervated from axons of cranial nerves whose cell bodies lie in the brain stem. Thus the olfactory epithelium and retina of the eye both contain projection neurons whose cell bodies are located in the peripheral sensory structure and are connected to the central nervous system via nerves that do not pass through the brain stem.
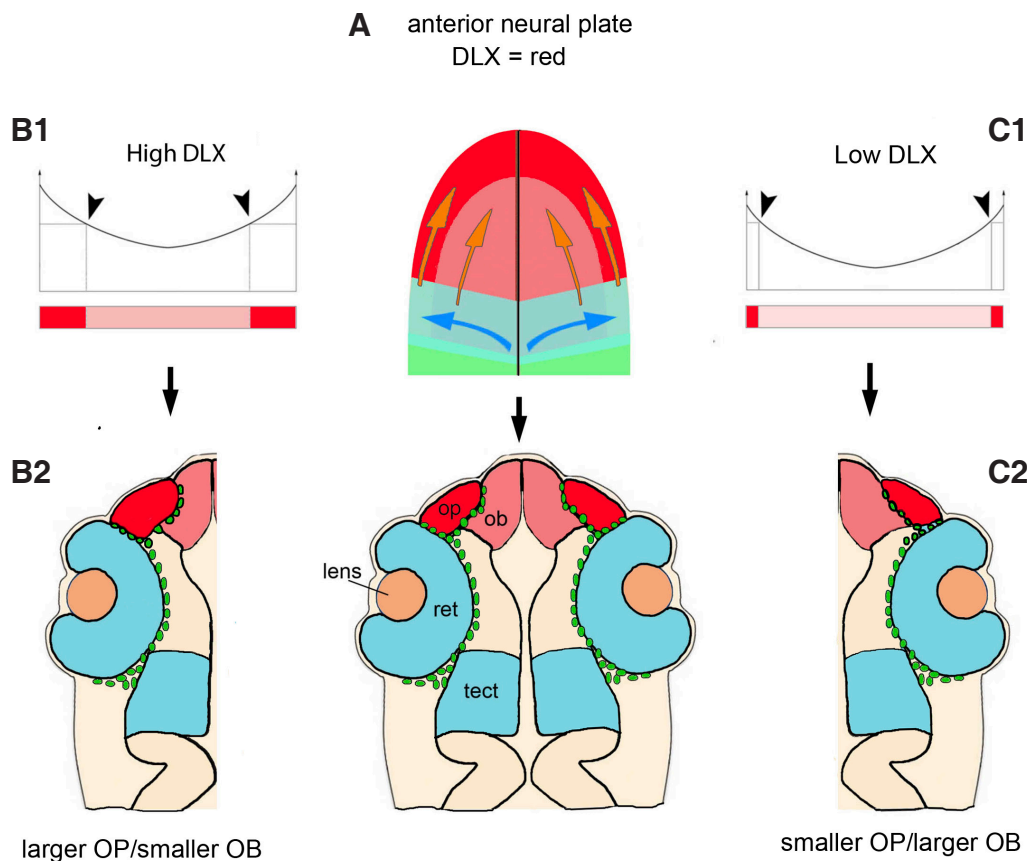
Dlx and patterning the anterior neural plate
The homeobox-containing family of DLX transcription factors plays a role in patterning various aspects of the invertebrate and vertebrate body plan. *Dlx3* is a homeodomain transcription factor in vertebrates, related to *Distal- less* in *Drosophila*. In vertebrates Dlx homeobox genes exist as multiple pairs of physically linked genes that have a high level of overlap in their expression patterns (Quint *et al.*, 2000; Zerucha *et al.*, 2000). The Dlx homeobox genes pattern the anterior neural plate, where the specific set of dlx genes are animal dependent. In chick (Pera and Kessel 1999; Zhu H, Bendall 2006), mouse (Long *et al.*, 2003; Parrilla *et al.*, 2016), and *Xenopus* (Franco *et al.*, 2001) the *dlx* genes are important in patterning both the peripheral (OE) and central (OB) olfactory system.

Previously we have shown that the OPs arise from the border of the neural plate in the region expressing high levels of *dlx3* (Whitlock and Westerfield, 2000) (Whitlock *et al.*, 2003) (Torres-Paz and Whitlock, 2014). Subsequently using the a *six4b:mCherry* reporter line as well as *six4b* in *situs* (Harden *et al.*, 2012) combined with the anti-dlx3b antibody we showed that Six4b:mCherry does not label the entirety of the *dlx3b* domain. Within OP field the anterior most region of the neural plate expresses both Dlx3 and Six4b:mCherry (Harden *et al.,* 2012; Fig. 1C) but only Dlx3 is expressed in the posterior domain. Likewise here we have shown that Sox3:GFP positive cells localize to the anterior region of the Dlx3b domain but not the posterior domain. These observations suggest that perhaps the anterior region of the OP domain generates different cell types and potentially the Six4b:mCherry domain is the source of support cells. Furthermore the domains may correspond to neurogenic domains where the anterior region generates the first neurons extending into the CNS (Whitlock and Westerfield, 1998, 2000).

In zebrafish *dlx3* expression in evident in wholemount embryos at 100% epiboly, thus the end of gastulation, indicating the pattern is initiated during gastrulation by upstream regulatory factors such as BMP (Luo *et al.*, 2001). The overexpression of *dlx3b* via mRNA injections proved difficult with low survivorship. Additionally, the importance of *dlx* as an instructive gene delineating the limit of the neural plate (Akimenko *et al.*, 1994) may be reflected in the lethality and altered morphology of our mRNA over-expression studies. A phenotype we observed in the over expression studies was a larger telencephalic ventricle with apparently thinner ventricle walls. In contrast to the animals scored at 24 hpf, *dlx3b* mRNA injected animals scored at 5 dpf (Fig. 7) showed a small but significant increase the size of the OE suggesting that the higher level of *dlx3b* could drive a proportion of precursor cells into the OP fate (Fig. 8, A, B), although more markers are needed to more thoroughly investigate the effects on over-expression.

It was previously shown that loss of function of *dlx3b*, and its functional paralogue *dlx4b* (*dlx3b/4b*), produce a disruption in the

A   anterior neural plate
DLX = red

B1   High DLX

C1   Low DLX

B2

larger OP/smaller OB

C2

smaller OP/larger OB

op, ob, lens, ret, tect

Fig. 8. Model: Distal-less (DLX) regulates the balance between central and peripheral olfactory precursors. (A) *DLX proteins are expressed at different levels in the olfactory field, with high levels in the periphery (dark red) and low levels towards the midline (pale red). Specific threshold levels of Dlx3b (arrowheads) are required in precursors to acquire placodal fates and telencephalic fates.* **(B1)** *Increasing levels of DLX will expand peripheral domain (dark red) resulting in larger OP (B2, dark red) and decreased OB (pale red) size.* **(C1)** *Reducing levels of DLX will decrease peripheral domain (dark red) resulting in a smaller OP (C2, dark red) and increased OB (pale red) size.*

development of otic vesicle and OP (Solomon and Fritz, 2002) although no phenotypes were reported in the CNS. Here we took advantage of one of the useful characteristics of morpholinos namely the ability to decrease (knock-down) protein expression. The results support our model Fig. 8) in that for *emx3*, important in patterning the OB/Tel the expression domain was expanded apparently at the expense of the OPs suggesting that the gradient decrease drives a greater proportion of precursor cells into the OB/Tel fate (Fig. 8, A, C).

Crossing the great divide: continuity of central and peripheral precursors

The clones of cells we observed extending across the morphological boundaries of the OB and OE reflect an intimate association of the progenitors in the neurectoderm before the formation of the neural tube. These clones (Fig. 2, A, C, D) were in the anterior two-thirds of the OP as were multiple groups of cell (Supplemental Movie #2). In contrast in one case (Fig. 2, D), a second clone was observed in the posterior OP, perhaps reflecting regional differences in cells types reflected by combinatorial expression of Dlx3b/Six4b:mCh (anterior domain) and only Dlx3b (posterior domain). To date the specific identities of these cells are unknown, but future studies will allow us to label more cells and track them for longer developmental time periods to discern their ultimate phenotype. The extensions displayed by the cells in the clones are similar to results from a recent study showing that during convergence of OP precursors there are already differentiating neurons establishing axonal contacts with the prospective OB (Breau *et al.*, 2017). The laminin "boundary" that eventually

develops is associated with the anterior migration of neural crest cells that will form the physical border (cribriform plate) dividing the OE from the bulb, just as neural crest derived bone (orbit of the eye) divide the retina from its central target in the brain.

The olfactory sensory system

The olfactory sensory system is the most unusual of the sensory systems in vertebrates because of not only its high levels of neurogenesis through life of both central and peripheral neurons, but also the continuity of meningeal covering that extends from the CNS along the olfactory nerves to the OE, a feature that is also shared with the optic nerve. A final curious characteristic of the olfactory sensory system is that the glia have characteristics of both CNS glial types and PNS glia types: the olfactory nerve is populated by unique type of non-myelinating glia, the olfactory ensheathing cells that possess a mixture of Schwann cell and astrocytic features and have been alternately described as arising from the olfactory placode (Doucette, 1991; Figueiredo *et al.*, 2011) and/or neural crest (Jacob, 2015). Thus the olfactory sensory epithelia of the PNS have many characteristics that are attributed to the CNS causing one to re-examine more closely the developmental origin of the OPs.

Conclusion/Future: Here we have shown that the OP/OB develop a coordinated manner from a continuous neurectoderm patterned during gastrulation These data support the emerging idea that not all placodes are the same and importantly, that the olfactory sensory system has very special characteristics: a meningeal covering and non-brainstem connection similar to the optic nerve, glia with characteristics distinct from other sensory

systems, and a class of sensory neurons whose first synapse lies within the CNS. Future studies will help us to better understand both the development and evolution of this most amazing sensory system in vertebrates.

Materials and Methods

Animals

Zebrafish were maintained in a re-circulating system (Aquatic Habitats Inc, Apopka, FL) at 28°C on a light-dark cycle of 14 and 10 hours respectively. Wild-type (WT) fish of the Cornell strain (derived from Oregon AB) were used. All protocols and procedures employed were reviewed and approved by the Institutional Committee of Bioethics for Research with Experimental Animals, University of Valparaiso (#BA084-2016). Embryos were obtained from natural spawnings in laboratory conditions and raised at 28.5°C in Embryo medium as described previously (Westerfield, 2007). Staging was done according to Kimmel *et al.,* 1995 (Kimmel *et al.*, 1995).

Transgenic lines: *six4b:mCherry* (Harden *et al.*, 2012), *SOX3Hs8a:GFP* (*sox3:GFP;* (Navratilova *et al.*, 2009) which was generated using a partial enhancer elements of the human *sox3* gene driving GFP expression, *HuC:GFP* (Park *et al.*, 2000), *omp:YFP*, *omp:RFP* (Sato *et al.*, 2005) and *sox10:mRFP* (Kucenas *et al.*, 2008) were used to visualize specific cell types.

Morpholino oligo (MO) injections

MOs were designed previously (Solomon and Fritz, 2002) and obtained from Gene Tools. As control we used the corresponding 5-nucleotides mismatch MOs (mmMOs). MOs sequences were:

*dlx3b*MO, 5'-ATATGTCGGTCCACTCATCCTTAAT-3' (GenBank #NM_131322);

*dlx3b*mm, 5'-ATtTcTCGcTCCACTgATgCTTAAT-3';

*dlx4b*MO, 5'-TAACCGTCAAGTCCATAAAGCCCGA-3' (GenBank #BC092714).;

*dlx4b*mm, 5'-TAAgCcTCAAcTCgATAAAcCCCGA-3'

MOs were re-suspended in autoclaved water at a final concentration of 1 mM (41.5 ng/nl). A total amount of 16 ng of *dlx3b/4b* MOs or mmMOs pre-mixed (8 ng each) in 5nL with 1% phenol red was injected in one-four cells stage embryos. Injection pipettes were pulled using borosilicate capillary glass with microfilament (OD=1.2mm, ID=0.94 mm, 10 cm length) on a Sutter Puller P-2000 (Sutter instruments). The same pipettes were used for mRNA injections. The phenotypes of the embryos where dlx3b/4b proteins were reduced were in agreement with previously described phenotypes of ((Solomon and Fritz, 2002); Fig. 4E-G).

Immunocytochemistry

Staged embryos were fixed in 4% paraformaldehyde diluted in 0.1M phosphate buffer with 0.15 mM CaCl$_2$ for 5 hours at room temperature, and then permeabilized in acetone at -20°C for 7 min. After 3 washes in 0.1M phosphate buffer embryos were incubated in block solution (0.1M phosphate buffer, 1% dimethylsulfoxide [DMSO], 0.5% Triton X-100, 2% bovine serum and 2% goat serum) and then incubated with the primary antibodies (diluted in block solution) for 5 hours at room temperature. After three washes during 2 hours, embryos were incubated in secondary antibodies over-night at 4°C. Embryos were rinsed in 0.1 M phosphate buffer and 1% DMSO 3 times for 1 hr and DNA stained for DAPI (1 mg/ml, Sigma) overnight. Primary antibodies used were anti-GFP (mouse 1:500, Life Technologies), anti-GFP (rabbit 1:1000, Life Technologies), anti-Laminin (rabbit 1:200, Sigma), Anti-mCherry, (mouse 1:250, Abcam), anti-Phosphorylated Histone H3, PH3 (rabbit 1:1000, Millipore), anti-RFP (rabbit 1:500, Invitrogen), anti-Tyrosine hydroxylase, TH (mouse 1:50, DSHB), and Anti-Zrf1, recognizing an epitope in the GFAP protein, (mouse 1:250 ZIRC). Secondary antibodies used were Dylight488 conjugated anti-mouse, anti-rabbit (goat 1:500, Jackson Immuno Research), Alexa568 conjugated anti mouse and anti-rabbit (goat 1:500, Molecular Probes), Cy5 conjugated anti-rabbit (Goat 1:500, Jackson Immuno Research).

In situ hybridization

Embryos were fixed in phosphate-buffered (100 mM) 4% paraformaldehyde (PFA 4%). *In situ* hybridization was performed as described in Thisse *et al.,* 1993, using single-stranded RNA probes labeled with digoxigenin-UTP (Roche, Mannheim, Germany). The *emx1* and *emx3* probes were generated using plasmids provided by the Westerfield lab, linearized with BamHI (New England Biolabs) and transcribed with T3 RNA Polimerase (mMessage mMachine System, Ambion).

mRNA injections

G*ap43-GFP* construct (gift from M. Concha lab, Universidad de Chile, Chile) was injected as circular DNA. *dlx3b* expression vector (a gift from Dr. Andreas Fritz, Emory University, USA) was linearized with KpnI and synthetic mRNA was produced using T3 RNA polymerase (mMessage mMachine System, Ambion). Embryos at one to four cell stages were injected with an amount of 150–200 pg (5-10 nL) of mRNA with 1% phenol red was injected per embryo. *dlx3b* mRNA injection: Embryos were injected at one to two cell stage with 10-20 pg (2-5 nL) of *dlx3b* mRNA with 1% phenol red per embryo. In clutches of embryos injected with *dlx3b* mRNA mortality was observed in 50% of the embryos, others show phenotypes indicating toxicity (edema of the heart) and defects in gastrulation indicating the high levels of *dlx3* expression may disrupt normal gastrulation.

Imaging and data analyses

Fluorescently labeled embryos were analyzed in a Spinning Disc microscope Olympus BX-DSU (Olympus Corporation, Shinjuku-ku, Tokyo, Japan). Images were acquired with an ORCA IR2 Hamamatsu camera (Hamamatsu Photonics, Higashi-ku, Hamamatsu City, Japan) using the Olympus Cell-R software (Olympus Soft Imaging Solutions, Munchen, Germany). Raw images were processed for deconvolution using the software AutoQuantX 2.2.2 (Media Cybernetics, Bethesda, MD) and analyzed in Fiji (National Institutes of Health, Bethesda, MD). For volume measurements we used the Measure Stack plug-in (Optinav Inc.) and for counting cells we used the Cell Counter plug-in. For statistical analysis the Unpaired t-test (Prism Graph) was used. Time lapse movies were made by capturing Z-stack every 2-3μm in a total depth of 40-60 μm every 10 minutes. Movies were assembled with Fiji. Quantification of the area expressing *emx1* or *emx3* at 24 hpf was done using CombineZP software (2015) where serial images from each embryo where measured and the area calculated.

References

AKIMENKO, M.A., EKKER, M., WEGNER, J., LIN, W., WESTERFIELD, M., (1994). Combinatorial expression of three zebrafish genes related to distal-less: part of a homeobox gene code for the head. *J Neurosci* 14: 3475-3486.

ANGELES FERNANDEZ-GIL, M., PALACIOS-BOTE, R., LEO-BARAHONA, M., MORA-ENCINAS, J.P., (2010). Anatomy of the brainstem: a gaze into the stem of life. *Semin Ultrasound CT MR* 31: 196-219.Begbie, J., Ballivet, M., Graham, A., (2002). Early steps in the production of sensory neurons by the neurogenic placodes. *Mol Cell Neurosci* 21: 502-511.

BEGBIE, J., GRAHAM, A., (2001). The ectodermal placodes: a dysfunctional family. *Philos Trans R Soc Lond B Biol Sci* 356: 1655-1660.

BREAU, M.A., BONNET, I., STOUFFLET, J., XIE, J., DE CASTRO, S., SCHNEIDER-MAUNOURY, S., (2017). Extrinsic mechanical forces mediate retrograde axon extension in a developing neuronal circuit. *Nat Commun* 8: 282.

CAVODEASSI, F., IVANOVITCH, K., WILSON, S.W., (2013). Eph/Ephrin signalling

maintains eye field segregation from adjacent neural plate territories during forebrain morphogenesis. *Development* 140: 4193-4202.

CHAPMAN, S.C., SCHUBERT, F.R., SCHOENWOLF, G.C., LUMSDEN, A., (2002). Analysis of spatial and temporal gene expression patterns in blastula and gastrula stage chick embryos. *Dev Biol* 245: 187-199.

DEE, C.T., HIRST, C.S., SHIH, Y.H., TRIPATHI, V.B., PATIENT, R.K., SCOTTING, P.J., (2008). Sox3 regulates both neural fate and differentiation in the zebrafish ectoderm. *Dev Biol* 320: 289-301.

DOUCETTE, R., (1991). PNS-CNS transitional zone of the first cranial nerve. *J Comp Neurol* 312: 451-466.

ESTERBERG, R., FRITZ, A., (2009). dlx3b/4b are required for the formation of the preplacodal region and otic placode through local modulation of BMP activity. *Dev Biol* 325: 189-199.

FAVRE, J.J., CHAFFANJON, P., PASSAGIA, J.G., CHIROSSEL, J.P., (1995). Blood supply of the olfactory nerve. Meningeal relationships and surgical relevance. *Surg Radiol Anat* 1995;17: 133-138.

FIGUEIREDO, M., LANE, S., TANG, F., LIU, B.H., HEWINSON, J., MARINA, N., KASYMOV, V., SOUSLOVA, E.A., CHUDAKOV, D.M., GOURINE, A.V., TESCHEMACHER, A.G., KASPAROV, S., (2011). Optogenetic experimentation on astrocytes. *Exp Physiol* 96: 40-50.

FRANCO, M.D., PAPE, M.P., SWIERGIEL, J.J., BURD, G.D., (2001). Differential and overlapping expression patterns of X-dll3 and Pax-6 genes suggest distinct roles in olfactory system development of the African clawed frog *Xenopus laevis. J Exp Biol* 204: 2049-2061.

GALEANO, C., QIU, Z., MISHRA, A., FARNSWORTH, S.L., HEMMI, J.J., MOREIRA, A., EDENHOFFER, P., HORNSBY, P.J., (2018). The Route by Which Intranasally Delivered Stem Cells Enter the Central Nervous System. *Cell Transplant* 27: 501-514.

HARDEN, M.V., PEREIRO, L., RAMIALISON, M., WITTBRODT, J., PRASAD, M.K., MCCALLION, A.S., WHITLOCK, K.E., (2012). Close association of olfactory placode precursors and cranial neural crest cells does not predestine cell mixing. *Dev. Dyn.* 241: 1143-1154.

HOLZSCHUH, J., RYU, S., ABERGER, F., DRIEVER, W., (2001). Dopamine transporter expression distinguishes dopaminergic neurons from other catecholaminergic neurons in the developing zebrafish embryo. *Mech Dev* 101: 237-243.

IVANOVITCH, K., CAVODEASSI, F., WILSON, S.W., (2013). Precocious acquisition of neuroepithelial character in the eye field underlies the onset of eye morphogenesis. *Dev Cell* 27: 293-305.

JACOB, C., (2015). Transcriptional control of neural crest specification into peripheral glia. *Glia* 10: 22816.

JACOBSON, A.G., (1966). Inductive processes in embryonic development. *Science* 152: 25-34.

JOHNSTON, J.B., (1909). The morphology of the forebrain vesicle in vertebrates. *J Comp Neurol Psychol* 19: 457–539.

KAWAHARA, A., DAWID, I.B., (2002). Developmental expression of zebrafish emx1 during early embryogenesis. *Gene Expr Patterns* 2: 201-206.

KIMMEL, C.B., BALLARD, W.W., KIMMEL, S.R., ULLMANN, B., SCHILLING, T.F., (1995). Stages of embryonic development of the zebrafish. *Dev Dyn* 203: 253-310.

KLEIN, S.L., GRAZIADEI, P.P., (1983). The differentiation of the olfactory placode in *Xenopus laevis*: a light and electron microscope study. *J Comp Neurol* 217: 17-30.

KUCENAS, S., TAKADA, N., PARK, H.C., WOODRUFF, E., BROADIE, K., APPEL, B., (2008). CNS-derived glia ensheath peripheral nerves and mediate motor root development. *Nat Neurosci* 11: 143-151.

LEVINE, C., MARCILLO, A., (2008). Origin and endpoint of the olfactory nerve fibers: as described by Santiago Ramon y Cajal. *Anat Rec (Hoboken)* 291: 741-750.

LONG, J.E., GAREL, S., DEPEW, M.J., TOBET, S., RUBENSTEIN, J.L., (2003). DLX5 regulates development of peripheral and central components of the olfactory system. *J Neurosci* 23: 568-578.

LUO, T., MATSUO-TAKASAKI, M., LIM, J.H., SARGENT, T.D., (2001). Differential regulation of Dlx gene expression by a BMP morphogenetic gradient. *Int J Dev Biol* 45: 681-684.

MACDONALD, R.B., DEBIAIS-THIBAUD, M., TALBOT, J.C., EKKER, M., (2010). The relationship between dlx and gad1 expression indicates highly conserved genetic pathways in the zebrafish forebrain. *Dev Dyn* 239: 2298-2306.

NAVRATILOVA, P., FREDMAN, D., HAWKINS, T.A., TURNER, K., LENHARD, B.,

BECKER, T.S., (2009). Systematic human/zebrafish comparative identification of cis-regulatory activity around vertebrate developmental transcription factor genes. *Dev Biol* 327: 526-540.

O'RAHILLY, R., MULLER, F., (1986). The meninges in human development. *J Neuropathol Exp Neurol* 45: 588-608.

PARK, H.C., HONG, S.K., KIM, H.S., KIM, S.H., YOON, E.J., KIM, C.H., MIKI, N., HUH, T.L., (2000). Structural comparison of zebrafish Elav/Hu and their differential expressions during neurogenesis. *Neurosci Lett* 279: 81-84.

PARRILLA, M., CHANG, I., DEGL'INNOCENTI, A., OMURA, M., (2016). Expression of homeobox genes in the mouse olfactory epithelium. *J Comp Neurol* 524: 2713-2739.

PATTHEY, C., GUNHAGA, L., (2014). Signaling pathways regulating ectodermal cell fate choices. *Exp Cell Res* 321: 11-16.

PATTHEY, C., SCHLOSSER, G., SHIMELD, S.M., (2014). The evolutionary history of vertebrate cranial placodes--I: cell type evolution. *Dev Biol* 389: 82-97.

PIEPER, M., EAGLESON, G.W., WOSNIOK, W., SCHLOSSER, G., (2011). Origin and segregation of cranial placodes in *Xenopus laevis. Dev Biol* 360: 257-275.

QUINT, E., ZERUCHA, T., EKKER, M., (2000). Differential expression of orthologous Dlx genes in zebrafish and mice: implications for the evolution of the Dlx homeobox gene family. *J Exp Zool* 288: 235-241.

ROBU, M.E., LARSON, J.D., NASEVICIUS, A., BEIRAGHI, S., BRENNER, C., FARBER, S.A., EKKER, S.C., (2007). p53 activation by knockdown technologies. *PLoS Genet* 3: e78.

SANCHEZ-ARRONES, L., SANDONIS, A., CARDOZO, M.J., BOVOLENTA, P., (2017). Adenohypophysis placodal precursors exhibit distinctive features within the rostral preplacodal ectoderm. *Development* 144: 3521-3532.

SATO, Y., MIYASAKA, N., YOSHIHARA, Y., (2005). Mutually exclusive glomerular innervation by two distinct types of olfactory sensory neurons revealed in transgenic zebrafish. *J Neurosci* 25: 4889-4897.

SCHILLE, C., SCHAMBONY, A., (2017). Signaling pathways and tissue interactions in neural plate border formation. *Neurogenesis (Austin)* 4: e1292783.

SCHLOSSER, G., (2006). Induction and specification of cranial placodes. *Dev Biol* 294: 303-351. Epub 2006 May 2003.

SCHLOSSER, G., (2010). Making senses development of vertebrate cranial placodes. *Int Rev Cell Mol Biol* 283: 129-234.

SCHLOSSER, G., AHRENS, K., (2004). Molecular anatomy of placode development in *Xenopus laevis. Dev Biol* 271: 439-466.

SCHLOSSER, G., PATTHEY, C., SHIMELD, S.M., (2014). The evolutionary history of vertebrate cranial placodes II. Evolution of ectodermal patterning. *Dev Biol* 389: 98-119.

SEN, S., REICHERT, H., VIJAYRAGHAVAN, K., (2013). Conserved roles of ems/Emx and otd/Otx genes in olfactory and visual system development in *Drosophila* and mouse. *Open Biol* 3: 120177.

SJODAL, M., EDLUND, T., GUNHAGA, L., (2007). Time of exposure to BMP signals plays a key role in the specification of the olfactory and lens placodes ex vivo. *Dev Cell* 13: 141-149.

SOLOMON, K.S., FRITZ, A., (2002). Concerted action of two dlx paralogs in sensory placode formation. *Development* 129: 3127-3136.

SOLOMON, K.S., KWAK, S.J., FRITZ, A., (2004). Genetic interactions underlying otic placode induction and formation. *Dev Dyn* 230: 419-433.

STAUDT, N., GIGER, F.A., FIELDING, T., HUTT, J.A., FOUCHER, I., SNOWDEN, V., HELLICH, A., KIECKER, C., HOUART, C., (2019). Pineal progenitors originate from a non-neural territory limited by FGF signalling. *Development* 146: dev.171405.

TORRES-PAZ, J., WHITLOCK, K.E., (2014). Olfactory sensory system develops from coordinated movements within the neural plate. *Dev Dyn* 243: 1619-1631.

TREVARROW, B., MARKS, D.L., KIMMEL, C.B., (1990). Organization of hindbrain segments in the zebrafish embryo. *Neuron* 4: 669-679.

VARGA, Z.M., WEGNER, J., WESTERFIELD, M., (1999). Anterior movement of ventral diencephalic precursors separates the primordial eye field in the neural plate and requires cyclops. *Development* 126: 5533-5546.

WALKER, H.K., (1990). Cranial Nerve I: The Olfactory Nerve Boston: Butterworths.

WESTERFIELD, M., (2007). The zebrafish book: A guide for the laboratory use of zebrafih (Danio rerio). University of Oregon Press, Eugene OR USA.

WHITLOCK, K.E., (2004). A new model for olfactory placode development. *Brain Behav Evol* 64: 126-140.

WHITLOCK, K.E., (2008). Developing a sense of scents: plasticity in olfactory placode formation. *Brain Res Bull* 75: 340-347.

WHITLOCK, K.E., (2015). The loss of scents: Do defects in olfactory sensory neuron development underlie human disease? *Birth Defects Res C Embryo Today* 105: 114-125.

WHITLOCK, K.E., WESTERFIELD, M., (1998). A transient population of neurons pioneers the olfactory pathway in the zebrafish. *J Neurosci* 18: 8919-8927.

WHITLOCK, K.E., WESTERFIELD, M., (2000). The olfactory placodes of the zebrafish form by convergence of cellular fields at the edge of the neural plate. *Development* 127: 3645-3653.

WHITLOCK, K.E., WOLF, C.D., BOYCE, M.L., (2003). Gonadotropin-releasing hormone (GnRH) cells arise from cranial neural crest and adenohypophyseal regions of the neural plate in the zebrafish, Danio rerio. *Dev Biol* 257: 140-152.

ZERUCHA, T., STUHMER, T., HATCH, G., PARK, B.K., LONG, Q., YU, G., GAMBAROTTA, A., SCHULTZ, J.R., RUBENSTEIN, J.L., EKKER, M., (2000). A highly conserved enhancer in the Dlx5/Dlx6 intergenic region is the site of cross-regulatory interactions between Dlx genes in the embryonic forebrain. *J Neurosci* 20: 709-721.

Further Related Reading, published previously in the *Int. J. Dev. Biol.*

From so simple a beginning – what amphioxus can teach us about placode evolution
Gerhard Schlosser
Int. J. Dev. Biol. (2017) 61: 633-648
https://doi.org/10.1387/ijdb.170127gs

Mechanisms of cranial placode assembly
Marie Anne Breau and Sylvie Schneider-Maunoury
Int. J. Dev. Biol. (2014) 58: 9-19
https://doi.org/10.1387/ijdb.130351mb

Six1 is indispensable for production of functional progenitor cells during olfactory epithelial development
Keiko Ikeda, Ryoichiro Kageyama, Yuko Suzuki and Kiyoshi Kawakami
Int. J. Dev. Biol. (2010) 54: 1453-1464 (10.1387/ijdb.093041ki)

Cloning and developmental expression of the soxB2 genes, sox14 and sox21, during Xenopus laevis embryogenesis
Doreen D. Cunningham, Zhuo Meng, Bernd Fritzsch and Elena Silva Casey
Int. J. Dev. Biol. (2008) 52: 999-1004 (10.1387/ijdb.082586dc)

Multiple functions of Dlx genes.
G R Merlo, B Zerega, L Paleari, S Trombino, S Mantero and G Levi
Int. J. Dev. Biol. (2000) 44: 619-626

THE INTERNATIONAL JOURNAL OF
DEVELOPMENTAL BIOLOGY
Volume 51 Nos. 6/7   2007
Ear Development

THE INTERNATIONAL JOURNAL OF
DEVELOPMENTAL BIOLOGY
Volume 53 Nos. 2/3   2009
Epigenetics & Development

THE INTERNATIONAL JOURNAL OF
DEVELOPMENTAL BIOLOGY
Volume 45 No. 1   Special issue
The Spemann-Mangold Organizer

THE INTERNATIONAL JOURNAL OF
DEVELOPMENTAL BIOLOGY
Volume 48 Nos. 8/9   Special Issue
Eye Development